In-Plane Silicon-On-Nothing Nanometer-Scale Resonant Suspended Gate MOSFET for In-IC Integration Perspectives — Source link ↗

Cedric Durand, Fabrice Casset, P. Renaux, N. Abele ...+6 more authors

Institutions: STMicroelectronics, Centre national de la recherche scientifique

Related papers:

- The resonant gate transistor

- Multi-gate vibrating-body field effect transistor (VB-FETs)

- The Resonant Body Transistor

- Amplified piezoelectric transduction of nanoscale motion in gallium nitride electromechanical resonators

- Ultra-Sensitive Capacitive Detection Based on SGMOSFET Compatible With Front-End CMOS Process

In-Plane Silicon-On-Nothing Nanometer-Scale Resonant Suspended Gate MOSFET for In-IC Integration Perspectives

Cédric Durand, Fabrice Casset, Philippe Renaux, Nicolas Abelé, Bernard Legrand, Denis Renaud, Eric Ollier, Pascal Ancey, Adrian M. Ionescu, Lionel Buchaillot

HAL Id: cea-00320837

https://hal-cea.archives-ouvertes.fr/cea-00320837

Submitted on 20 Sep 2008

In-Plane Silicon-On-Nothing Nanometer-Scale Resonant Suspended Gate MOSFET for In-IC Integration Perspectives

C. Durand, F. Casset, P. Renaux, N. Abelé, B. Legrand, D. Renaud,
E. Ollier, P. Ancey, A. M. Ionescu, and L. Buchaillot

Abstract—A 14-MHz in-plane nanoelectromechanical resonator based on a resonant-suspended-gate (RSG) MOSFET principle and integrated in a front-end process is demonstrated. The devices are in-plane flexural vibration mode beams ($L = 10$ μm, $w = 165$ nm, and $h = 400$ nm) with 120-nm gaps. This letter details the design and process flow fabrication steps. Then, the electrical device characteristics are demonstrated, comprising static and dynamic studies around the resonant frequency. Devices enable the comparison of a pure capacitive detection with the RSG-MOSFET-based detection on the same component, showing a 4.3-dB-huge peak. Due to its output signal amplification and in-IC integration potentialities, the RSG-MOSFET-based detection is ideal for any type of nanoelectromechanical structure displacement detection.

Index Terms—In-IC integration, in-plane resonator, nanometer-scale resonator, resonant suspended gate (RSG) MOSFET, silicon on nothing (SON).

I. INTRODUCTION

FOR THE first time, an in-plane nanoelectromechanical (NEM) resonator based on a resonant suspended gate (RSG) MOSFET principle [1], [2] and integrated in a front-end process is demonstrated. Advanced silicon-on-nothing (SON) technology [3] based on industrial 8-in tools is used to fabricate RSG-MOSFETs with high in-IC integration capabilities.

This letter reports on the design, fabrication process, measurement setup, and experimental results of a 14-MHz NEM resonator and compares a classic capacitive detection [4] with
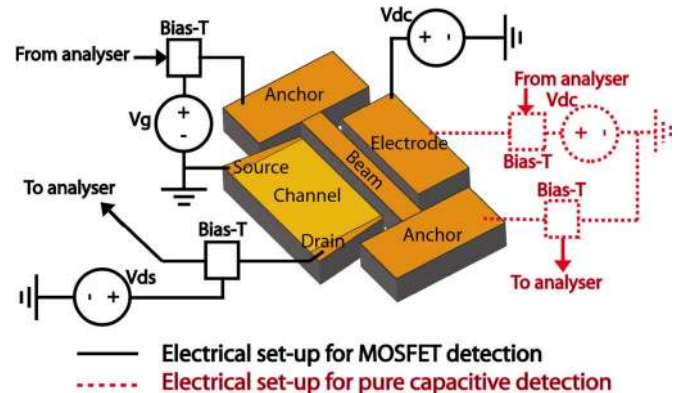
Fig. 1. Principle schematic and electrical characterization setup of the RSG-MOSFET device.

a MOSFET-based detection. Operational dc and vibrating characteristics of laterally excited nanogap RSG-MOSFETs are also reported for the first time. The proposed process and fabricated resonators enable the in-IC integration of off-chip modules such as time reference functions with significant cost, size, and consumption reduction [5].

II. DEVICE DESIGN AND FABRICATION

The lateral MOSFET is composed of a vibrating gate and a channel separated from the mobile gate by an insulator and an air gap (Fig. 1). Drain and source are placed in the same horizontal plane as the gate. The mobile-gate (beam) vibration at resonance frequency modulates the mobile charges of the MOS conductive channel formed along the lateral etched sidewall and, consequently, the drain current. The design and the proposed process enable the integration of both capacitive [4] and amplified detections using the MOSFET intrinsic gain (tailored by the transistor transconductance $i_{ds} = \nu_{gs} \times g_m$).

Devices were fabricated by using the SON technology [3] to achieve sub-100-nm gaps and 400-nm-thick single-crystal silicon resonators using only front-end processes [4], [6] and materials, ensuring the in-IC integration capabilities. The fabrication-process flow presented in [4] and [6] is resumed in Fig. 2. It starts with the patterning of active areas through a thermal SiO_2 layer. A SiGe sacrificial layer is then grown by selective epitaxy and followed by a low boron-doped (10^{16} at/cm^3) nonselective single-crystal silicon epitaxy. Phosphorous dopants are implanted (10^{19} at/cm^3) to define gate,
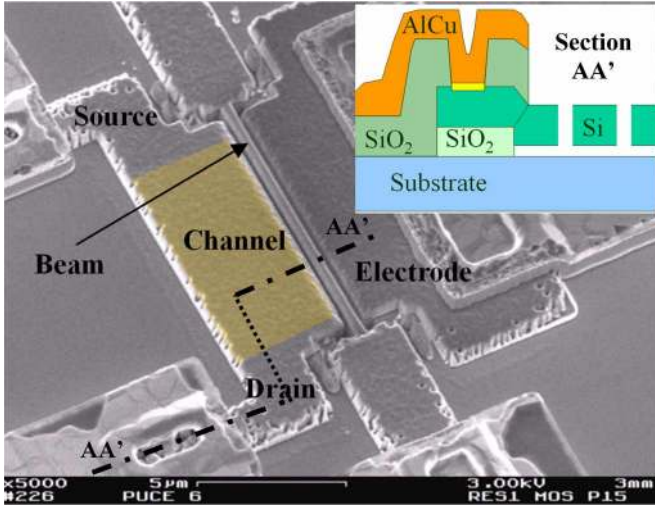
Fig. 2. Perspective SEM picture of a beam ($L = 10 \ \mu m$, $w = 165$ nm, and $d = 120$ nm).

source, and drain. E-beam lithography is used to define gaps and the resonator structure, leading to a 47-nm gap resolution. The 400-nm-thick silicon structural layer is then etched by an anisotropic plasma to define air gaps. After dopant diffusion and activation annealing steps, structures are released by an isotropic plasma etch of the SiGe sacrificial layer. The released structures were protected by a nonconformal SiO_2 deposition to allow metal pad deposition. Fig. 2 shows a picture of a suspended RSG-MOSFET.

III. MEASUREMENT SETUP

RF characterizations are performed by using an Agilent 8753E network analyzer. Fig. 1 shows the two measurement configurations for comparing capacitive and MOSFET detections on the same device.

For a capacitive-detection measurement [4], the transmitted signal through the resonator is measured between the vibrating beam and the electrode of the device. A bias voltage V_{dc} is applied on the electrode; the beam and the substrate are grounded to avoid any pull-in effect of the structure.

For a MOSFET-detection measurement, three bias voltages are applied: the electrode V_{dc}, the gate voltage V_g, and the drain voltage V_{ds}. Optimal V_g and V_{ds} values for dynamic characterization were extracted from the static MOSFET characteristics $I_d(V_g)$ shown in Fig. 3 as well as $I_d(V_{ds})$.

IV. EXPERIMENTAL RESULTS

Fig. 3 shows the static electrical $I_d(V_g)$ measured characteristics of the MOSFET transistor. The threshold voltage V_{th} is 2 V. An OFF-state leakage current of 0.1–1.3 μA depending quasi-linearly on V_{ds} is observable at $V_g = 0$ V. It is attributed to a photolithography misalignment when protecting channel from phosphorous implants. Indeed, channel surface was partially implanted on a few nanometer widths, generating a 2.1-MΩ short-circuit resistor in parallel of the transistor, explaining the high leakage current and its quasi-linear dependence on V_{ds}. Optimal operating points were defined from
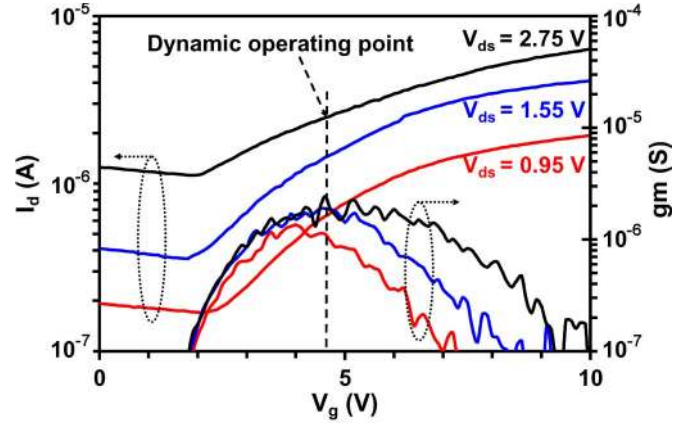

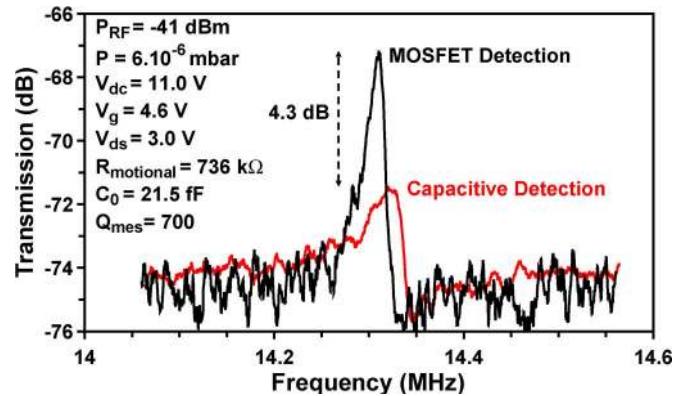Fig. 3. Static MOS characteristics $I_d(V_g)$ and $G_m(V_g)$.

Fig. 4. Capacitive- and MOSFET-detection comparison on the dynamic response of the NEMS ($L = 10 \ \mu m$, $w = 165$ nm, and $d = 120$ nm).

static characteristics: V_g being 4.6 V corresponding to the maximum of transconductance and V_{ds} being 3 V corresponding to the saturation region, with an OFF-state leakage of 1.4 μA.

Fig. 4 compares the resonant amplitude response between capacitive and MOSFET detections, on the same structure ($L = 10 \ \mu m$, $w = 165$ nm, and $d = 120$ nm). The fundamental resonance frequency was measured to be 14.33 and 14.31 MHz with capacitive and MOS detections, respectively. The slight discrepancy between the two measurements is explained by the different bias conditions of actuation between the MOS and capacitive detections. The frequency shift is mainly due to the MOSFET channel surface potential which is set to zero in the case of the capacitive detection. Measurements are in good agreement with mechanical analytical calculations and FEM simulations, giving 14.43 and 14.42 MHz, respectively, being independent of the detection principle. The extracted motional resistance R_m is 736 kΩ, and the C_0 capacitance is 21.5 fF. The MOSFET detection yields a +4.3 dB signal amplification compared with the capacitive detection due to the MOSFET intrinsic gain. This amplitude could be increased first by optimizing the transistor design (channel width/length ratio), hence enabling a higher g_m, and second by limiting the leakages. In this way, the SiGe layer has to be completely etched, and the SiO_2 insulation layer has to be thicker.
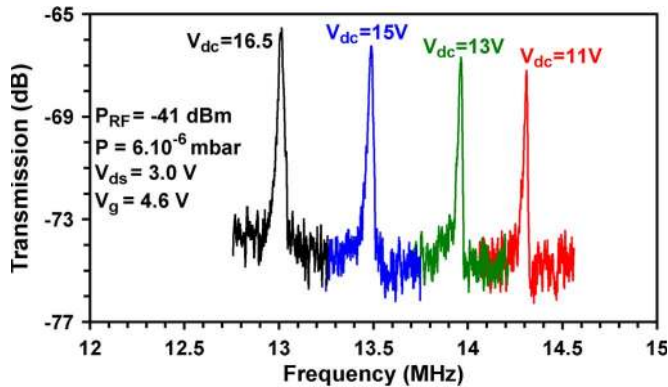
Fig. 5. Influence of V_{dc} variation on the dynamic response of the NEMS ($L = 10 \ \mu$m, $w = 165$ nm, and $d = 120$ nm) using the MOSFET detection.

Fig. 5 shows the influence of the beam polarization on the output signal using the MOSFET detection. Its amplitude increases with V_{dc} due to the larger beam vibration amplitude caused by the larger electrostatic excitation. The effect is also reinforced by the air-gap reduction induced by the increase in V_{dc}. On the other hand, the electrostatic field increases with V_{dc} and acts as a negative stiffness, shifting down the resonant frequency of 10% for a 5.5 V V_{dc} variation. The influence of V_{ds} on the device response was also investigated. Results show an increase in the resonant peak amplitude with V_{ds}, as predicted on static characteristics for a given V_g of 4.6 V, due to the increase in g_m with V_{ds}. Moreover, a V_{ds} variation from 2.0 to 3.5 V induces a 0.16% decrease in the resonant frequency. This effect is negligible regarding the shift induced by V_{dc}.

Dependence of resonators' behavior with environmental conditions was studied in [4] on similar devices. Resonant frequencies shift down quasi-linearly with temperature (from $-50\ °$C to $100\ °$C), giving a temperature coefficient of frequency of -32 ppm/$°$C. Quality factors were found to be maximum and constant at low pressure (< 1 Torr), whereas they decrease at higher pressures, showing that even for nanoscaled beams, air damping remains the major source of dissipation.

V. CONCLUSION

We fabricated and experimentally demonstrated, for the first time, a fully operational in-plane 14-MHz RSG-MOSFET resonator with intrinsic tunable amplification. The unique large gain, in terms of peak detection amplitude, makes this new device ideal for any type of NEM structure displacement detection. Future works will focus on reliability issues such as fatigue [7], packaging, and in-IC integration for industrial perspectives.

REFERENCES

[1] N. Abelé, R. Fritschi, K. Boucart, F. Casset, P. Ancey, and A. M. Ionescu, "Suspended-gate MOSFET: Bringing new MEMS functionality into solid-state MOS transistor," in *IEDM Tech. Dig.*, Washington, DC, Dec. 5–7, 2005, pp. 479–481.

[2] D. Grogg, D. Tsamados, N. D. Badila, and A. M. Ionescu, "Integration of MOSFET detection in MEMS resonators for improved output detection," in *Proc. Transducers*, Lyon, France, Jun. 10–14, 2007, pp. 1709–1712.

[3] S. Monfray, T. Skotnicki, Y. Morand, S. Descombes, M. Paoli, P. Ribot, A. Talbot, D. Dutartre, F. Leverd, Y. Le Friec, R. Pantel, M. Haond, D. Renaud, M.-E. Nier, C. Vizioz, D. Louis, and N. Buffet, "First 80 nm SON (Silicon-On-Nothing) MOSFETs with perfect morphology and high electrical performance," in *IEDM Tech. Dig*, Washington, DC, Dec. 3–5, 2001, pp. 2971–2974.

[4] C. Durand, F. Casset, B. Legrand, M. Faucher, P. Renaux, D. Mercier, D. Renaud, D. Dutartre, E. Ollier, P. Ancey, and L. Buchaillot, "Characterization of In-IC integrable in-plane nanometer scale resonators fabricated by a silicon on nothing advanced CMOS technology," in *Proc. MEMS*, Tucson, AZ, Jan. 13–17, 2008, pp. 1016–1019.

[5] C. T.-C. Nguyen, "Vibrating RF MEMS technology fuel for an integrated micromechanical circuit revolution?" in *Proc. Transducers*, Seoul, Korea, Jun. 5–9, 2005, pp. 243–246.

[6] C. Durand, F. Casset, P. Ancey, F. Judong, A. Talbot, R. Quenouillère, D. Renaud, S. Borel, B. Florin, and L. Buchaillot, "Silicon on nothing MEMS electromechanical resonator," in *Proc. DTIP*, Stresa, Italy, Apr. 25–27, 2007, pp. 326–331.

[7] A. George, A. Jacques, and M. Legros, "Low-cycle fatigue in silicon: Comparison with fcc metals," *Fatigue Fract. Eng. Mater. Struct.*, vol. 30, no. 1, pp. 41–56, Jan. 2007.